

짧은 전류 펄스를 이용한 전류 유도 자화 반전에서 에너지 장벽 분포의 효과

김우영 · 이경진*

고려대학교 신소재공학과, 서울시 성북구 안암동 5가 5-1, 136-713

(2011년 3월 28일 받음, 2011년 4월 11일 최종수정본 받음, 2011년 4월 11일 게재확정)

본 논문에서는 짧은 전류 펄스를 이용한 미소자기 소자에서의 전류 유도 자화 반전에 대한 매크로 스핀 시뮬레이션 연구를 수행하였다. 자화 반전 전류 분포에 있어서 에너지 장벽이 미치는 효과에 특별히 주목하였다. 자화 반전 전류의 크기 및 분포는 전류 펄스 폭의 감소에 따라 증가했다. 여기서 긴 전류 펄스 폭 영역에서는 에너지 장벽과 자화 반전 전류 분포 사이의 관계가 아레니우스-닐 법칙에 의해 서술된다. 하지만 짧은 전류 펄스 폭의 영역에서는 이 관계가 풀리지 않은 채로 남아있다. 이는 짧은 전류 펄스로 인한 자화 반전이 열적 활성화에 의해서가 아닌 세차 운동에 의해 좌우되기 때문이며, 이를 해결하는 데에 있어서 어려움이 발생한다. 그러므로 포커-플랑크 방정식을 풀어서 짧은 전류 펄스 영역에서의 자화 반전에 대한 정확한 공식을 얻어내는 것이 필요하며 이를 통해 짧은 전류 펄스 영역에서의 자화 반전 양상을 이해 할 수 있을 것으로 본다.

주제어 : 스피너달토크, 짧은 펄스에 의한 자화 반전

Effect of Energy Barrier Distribution on Current-Induced Magnetization Switching with Short Current Pulses

Woo-Yeong Kim and Kyung-Jin Lee*

Dept. of Materials Science and Engineering, Korea University, Seoul 136-713, Korea

(Received 28 March 2011, Received in final form 11 April 2011, Accepted 11 April 2011)

We performed macro-spin simulation studies of the current-induced magnetization reversal of nanomagnetic elements with short current pulses. A special attention was paid to the effect of the energy barrier on the switching current distribution. The switching current and its distribution increase with decreasing the current pulse-width. The relationship between the energy barrier and switching current distribution is described by the Arrhenius-Néel law at a long pulse-width regime. At a regime of short pulse-width, however, the relationship is left unaddressed. The difficulty to address this issue arises because the magnetization switching with a short current pulse is governed not by the thermal activation but by the precession motion. Therefore, an exact formulation for the short pulse regime by solving the Fokker-Plank equation is needed to understand the result.

Keywords: spin transfer torque, short-pulse switching

I. Introduction

Recently magnetization switching using spin transfer torque (STT) [1, 2] has received considerable interest because of the potential application for the magnetic devices such as magnetic random access memory (MRAM). From the application point of view, a fast magnetization switching

is required to obtain as high performance as the dynamic RAM (DRAM) has [3-6]. On the other hand, the magnetic cell size can have a distribution in real manufacturing processes. This distribution of the cell size is directly related to the energy barrier distribution and causes a reduction in the retention time of the stored information. It also causes the distribution of switching currents. In this work, we numerically investigated the dependence of the switching current distribution on the energy barrier at

*Tel: (02) 3290-3289, E-mail: kj_lee@korea.ac.kr

a short-pulse regime, which is important for the fast operation of MRAM cells.

II. Simulation Model

In this work, we performed macrospin simulations using Landau-Lifshitz-Gilbert equation with a spin torque term

$$\frac{d\mathbf{M}}{dt} = -\gamma \mathbf{M} \times \mathbf{H}_{eff} + \frac{\alpha}{M_S} \mathbf{M} \times \frac{d\mathbf{M}}{dt} + \frac{\gamma a_J}{M_S} \mathbf{M} \times (\mathbf{M} \times \mathbf{p}), \quad (1)$$

$$a_J = \frac{\hbar}{2eM_S} \frac{g}{t} J, \quad (2)$$

where γ is the gyromagnetic ratio, \mathbf{M} is the magnetization vector of the free layer, \mathbf{H}_{eff} is the effective magnetic field acting on the free layer, α ($= 0.01$) is the Gilbert damping constant, \mathbf{p} is the unit vector along the spin polarization direction, and M_S ($= 1000$ emu/cm 3) is the saturation magnetization of the free layer, a_J is the amplitude of the spin torque, g ($= 0.5$) is the spin-torque efficiency factor, t is the film thickness of the free layer, and J is the current density.

The free layer is assumed to have a length of L nm, a width of 60 nm, and a thickness of 3 nm. To vary the thermal stability factor ($= U_0/k_B T$) where U_0 is the thermal energy barrier, we varied the length of the cell (L) from 83 nm to 120 nm. Current pulse was applied with various pulse widths (τ) from 1 ns to 900 ns, and the operating temperature T was 300 K. To obtain the switching current distribution, we calculated more than 100 switching events for a given bias condition, and statistically analyzed the results.

III. Result and Discussion

Fig. 1(a) shows the switching probability (P_{SW}) versus applied current density ($J_{Applied}$) at cell length $L = 120$ nm. Fig. 1(b) and Fig. 1(c) show the averaged switching current density J at $P_{SW} = 50\%$ and the switching current density distribution with various current pulse-widths as a function of L respectively. Thermal stability factor $U_0/k_B T$ of the top axis is corresponding to L . Here, the switching current density distribution is defined by the full-width at half maximum (FWHM) of the curve of $dP_{SW}/d(J_{Applied})$ versus $J_{Applied}$. For a short τ , the averaged switching current density rapidly increases with decreasing τ , which is a well-known feature of the precessional switching induced by spin torque. The FWHM also increases with decreasing τ . The averaged switching current density at $\tau = 1$ ns is about 4 times larger than that at $\tau = 900$ ns, whereas the

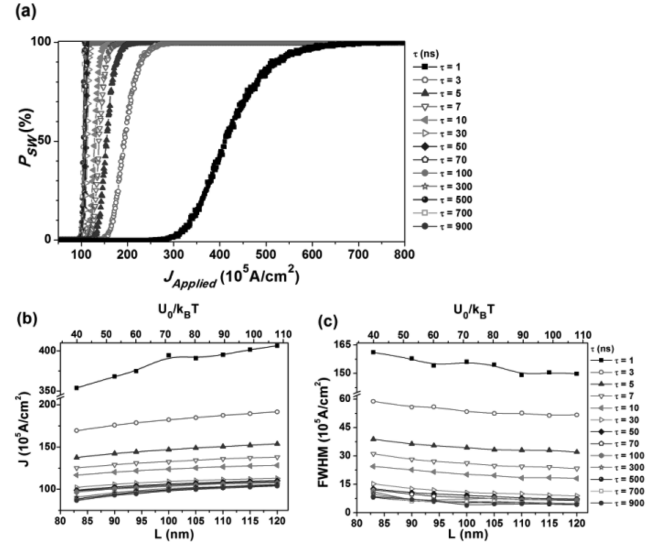


Fig. 1. (a) Switching probability (P_{SW}) versus applied current density ($J_{Applied}$) at cell length $L = 120$ nm and $T = 300$ K. (b) Averaged switching current density (J) versus cell length (L) and (c) FWHM versus cell length (L) with various current pulse widths at $T = 300$ K. The top horizontal axis is the thermal stability factor corresponding to the cell length of the bottom axis.

FWHM at $\tau = 1$ ns is about 30 times larger than that at $\tau = 900$ ns. It indicates that the precession switching affects the switching current density distribution more significantly than the averaged switching current density. We found that the FWHM slightly increases with decreasing L , which can be understood by the fact that a reduced energy

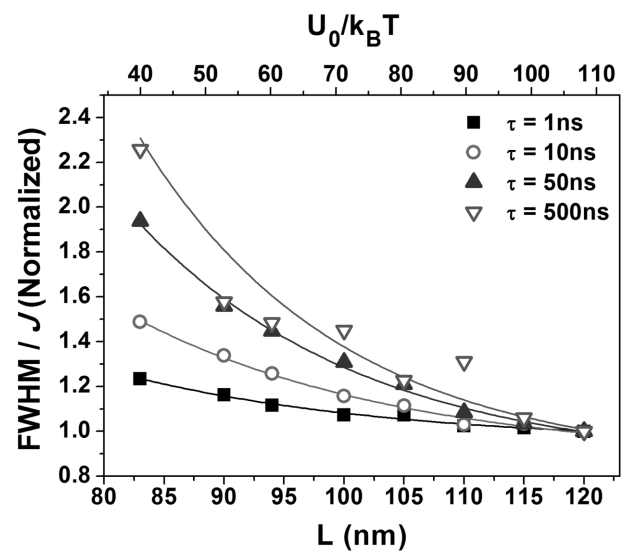


Fig. 2. Normalized ratio of full-width-at-half-maximum (FWHM) to J versus L at $T = 300$ K. All ratios are normalized with the value at $L = 120$ nm.

barrier causes a wider distribution of the switching current density. We also found that the averaged switching current density decreases with decreasing L . This can be understood by the following reason. A smaller L with the fixed width and thickness results in a smaller out-of-plane demagnetization field due to the relation between the demagnetization factors and the cell geometry.

Fig. 2 shows the ratio of the FWHM to the averaged current density. All the ratios are normalized by the data at $L = 120$ nm and each solid line is a non-linearly fitted line of each ratio. Although the absolute value of the FWHM is much larger with a shorter τ (Fig. 1), the normalized ratio with a shorter τ is less sensitive to the variation of the energy barrier than the ratio with a longer τ . With a longer current pulse width, the relative FWHM significantly changes with the variation of the cell length L , compared to the cases of shorter current pulse width. At $\tau = 500$ ns, the relative FWHM at $L = 83$ nm is more than twice as larger than that at $L = 120$ nm. At $\tau = 1$ ns, however, the relative FWHM changes only about 22% for the same change in the cell length. It indicates that the thermally activated switching is directly related to the size of the magnetic cell and is dominant at the long pulse-width regime. From the application point of view, the results show a prospect that the shape distribution of the magnetic cells in real manufacturing processes in the regime of short pulse-width spin current is less considerable than that in the regime of long pulse-width spin current.

For a long τ , the simulation results are in good agreement with following equation of the Arrhenius-Néel thermal decay of the switching probability

$$P_{SW} = 1 - \exp\left[-f_0\tau \exp\left(\frac{U_B}{k_B T}\right)\right], \quad (3)$$

$$U_B = U_0\left(1 - \frac{J}{J_C}\right), \quad (4)$$

where f_0 is the attempt frequency obtained by fitting numerical results of P_{SW} as a function of current pulse-width [7], and J_C is the zero temperature critical current density. Fig. 3 shows the averaged switching current density J as a function of the current pulse width $\log_{10}(\tau)$. Here each line (solid, dotted, and dashed-dotted) is a fit to the data using Eq. (3) with respect to L . However, at the regime of a short pulse width, the decaying equation is found to be unable to explain the simulation results. It is because the precessional switching dynamics induced by the spin current is more dominant than the thermally activated switching dynamics in this regime. To describe this regime the exact formulae by solving the Fokker-Plank equation are needed.

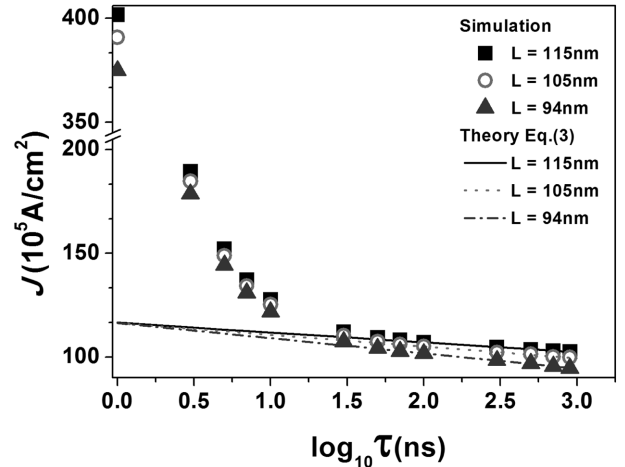


Fig. 3. J versus current pulse width $\log_{10}(\tau)$ with respect to L at $T = 300$ K. Solid, dotted, and dashed-dotted lines are fits to the data at a long pulse width regime.

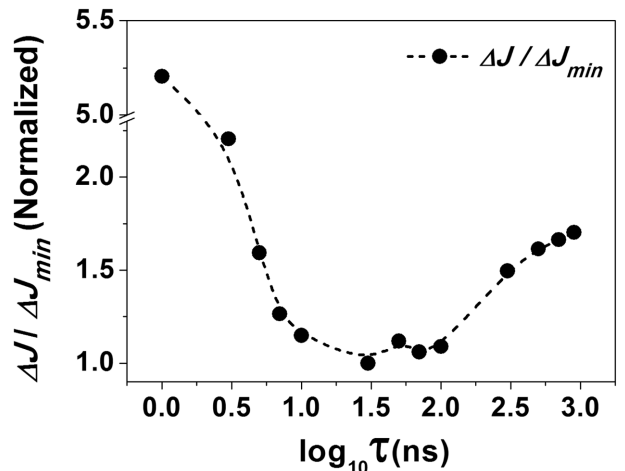


Fig. 4. Normalized ratio of J distribution ($\Delta J = J_{L=120} - J_{L=40}$) versus current pulse width $\log_{10}(\tau)$. All ratios are normalized by the minimum value of ΔJ .

As shown Fig. 4, we found that the distribution of the averaged switching current density ($\Delta J = J_{L=120} - J_{L=40}$) is relatively small at an intermediate pulse width regime ($10 \text{ ns} < \tau < 100 \text{ ns}$). ΔJ increases drastically with decreasing the current pulse width at $\tau < 10 \text{ ns}$. It is because the J at short pulse-width regime is affected by the precessional switching as described above. ΔJ also increases gradually with increase of the current pulse width at $\tau > 100 \text{ ns}$. In the region of long pulse width in Fig. 3, each slope of the fitted line slightly decreases with decreasing L . It is because the slope is proportional to the thermal stability factor. This indicates that the intermediate regime is less sensitive to the distribution of the energy barrier than other regimes. This regime also shows a relatively lower J than that of

the short pulse width region; in this regime, both spin torque precession motion and thermal activated motion have a synergistic interaction for the magnetization switching.

IV. Conclusion

We investigated the switching current density distribution of nanomagnetic cells at a short pulse-width regime and its relationship to the energy barrier distribution. We found that the switching current density distribution increases more significantly than the averaged switching current density as the pulse-width decreases. This result should be related to the precessional switching at a short pulse-width regime, implying that an exact formulation for a short pulse regime by solving the Fokker-Plank equation is needed to understand the result. We also found that the switching current density is less sensitive to the distribution of the energy barrier at the intermediate pulse regime, which exists in between the thermally activated switching regime and the precessional switching regime. This may provide a clue to find the optimal condition for the stable operation of high speed MRAMs.

Acknowledgement

This work was supported by IT R&D program of MKE/KEIT (Grant No 2009-F-004-01).

References

- [1] J. C. Slonczewski, *J. Magn. Magn. Mater.* **159**, L1 (1996).
- [2] L. Berger, *Phys. Rev. B* **54**, 9353 (1996).
- [3] D. Bedau, H. Liu, J. Z. Sun, J. A. Katine, E. E. Fullerton, S. Mangin, and A. D. Kent, *Appl. Phys. Lett.* **97**, 262502 (2010).
- [4] M. L. Schneider, M. R. Pufall, W. H. Rippard, and S. E. Russek, *Appl. Phys. Lett.* **90**, 092504 (2007).
- [5] A. A. Tulapurkar, T. Devolder, K. Yagami, P. Crozat, C. Chappert, A. Fukushima, and Y. Suzuki, *Appl. Phys. Lett.* **85**, 5358 (2004).
- [6] S. Kaka, M. R. Pufall, W. H. Rippard, T. J. Silva, S. E. Russek, J. A. Katine, M. Carey, *J. Magn. Magn. Mater.* **286**, 375 (2005).
- [7] H-J. Suh, C.-H. Heo, C.-Y. You, W.-J. Kim, T.-D. Lee, and K.-J. Lee, *Phys. Rev. B* **78**, 064430 (2008).